Initial deformation in a subduction thrust system: Polygonal normal faulting in the incoming sedimentary sequence of the Nankai subduction zone, Southwestern Japan.

A. S. Heffernan*[1], J. C. Moore[1], N. L. Bangs[2], G. F. Moore[3], T. H. Shipley[2]

1. Department of Earth Sciences, University of California Santa Cruz, 1156 High St., Santa Cruz, CA 95064
2. University of Texas Institute for Geophysics, 4412 Spicewood Springs Rd., Austin, TX 78759
3. Department of Geology and Geophysics, 1680 East West Rd., University of Hawaii, Honolulu, HI 96822

*corresponding author (adam_heffernan@aoageophysics.com)

Number of Words: 4362

ABSTRACT

3d seismic data from the Nankai margin provide detailed imagery documenting the onset of deformation at an active sediment-dominated accretionary prism, including a previously unmapped network of normal faults. The Nankai margin off southwest Japan is characterized by active subduction, seismogenesis, and a large accretionary prism with fold-and-thrust belt structure. Imbricate thrusting is the dominant structural style of the outer 20 km of the prism. This structural domain develops at the prism toe, where an incipient

imbricate thrust displays significant along-strike variability in dip, offset, and development of hanging wall anticlines.

Compressional deformation is preceded by normal faulting that initiates seaward of the trench axis. Seismic data in this area reveal a complex, intersecting pattern of normal faults within the incoming hemipelagic sediments. Underlying the faulted section is a high amplitude reflector interpreted as representing oceanic basement. This reflector contains elongate horsts and grabens oriented perpendicular to the margin interpreted as relict spreading center fabric.

Analysis of the orientation of normal faults within the Shikoku basin sequence shows a correlation between fault geometry and basement structure. This faulting is notably similar to layer-bound compaction faults, documented in the North Sea and elsewhere, attributed to both hydrofracturing and volumetric contraction of fine-grained sediments. Mapped normal faults may thus be the result of a combination of differential compaction of sediments above irregular, dipping oceanic basement and compactional dewatering seaward of the toe of the accretionary prism.

The Nankai Trough is the bathymetric expression of the convergent margin formed where the Philippine Sea Plate subducts beneath the southwest Japan arc. Convergence rates here are between 2 and 4 cm/yr [*Karig*, 1986; *Seno et al.*, 1993] (Figure 1). As subduction occurs a thick sequence of hemipelagic sediments and turbidites is accreted to the overriding plate. The resulting accretionary prism provides a record of subduction zone processes, including the development of classic fold-and-thrust belt structure, and mechanical and diagenetic processes associated with the accretion of young marine sediments.

The Nankai margin has been a focus of extensive, multinational scientific investigation in recent years. These investigations have included Ocean Drilling Program Legs 131, 190, and 196, [*Shipboard Scientific Party*, 1991; *Shipboard Scientific Party*, 2001; *Shipboard Scientific Party*, 2002; Mikada et al., 2002] multiple 2D and 3D seismic reflection surveys [*Aoki et al.*, 1982; *Moore et al.*, 1990], OBS surveys [*Kodaira et al.*, 2000], and various seafloor mapping surveys. Historical records describe frequent, massive earthquakes in the Nankai area from 684 AD to modern times. The 1946 Nankaido (M_s = 8.2) and 1944 Tonankai earthquakes (M_s = 8.0) are the most recent large earthquakes to occur in this area [*Ando*, 1975; *Ando*, 1991] and underscore the ongoing nature of seismic and tsunamigenic hazards here.

This study utilizes a 3D multichannel seismic (MCS) reflection survey collected off Muroto peninsula comprising an 8 by 80 km transect oriented perpendicular to the margin. This survey images the stratigraphy of the Shikoku Basin, the onset of compressional deformation, and landward approximately 60

km into the accretionary prism [*Moore et al.*, 2001a]. Structural characteristics of this accretionary system have been described in detail by previous work [Moore et al., 1990; Moore et al., 2001c]. This study utilizes 3D seismic data to document fine-scale structural variability in the earliest stages of deformation, a previously unmapped pattern of normal faults in the incoming sedimentary section, and underlying basement morphology. Normal fault geometry could not be determined from previously existing 2D seismic data, and may be characteristic of deformation found in other sediment-dominated subduction zones worldwide.

DATA ACQUISITION AND PROCESSING

The desire to understand the upper aseismic to seismic transition in subduction zones and associated earthquake hazard motivated the collection of the data used in this study . The effort was funded by the US National Science Foundation and equivalent agencies in Japan. Data were acquired aboard the Lamont-Doherty Earth Observatory's R/V Ewing during cruise EW9907-08, from June 18, 1999 to August 18, 1999. During this period 81 individual lines were shot, covering an 8 x 80 km transect oriented NW-SE across the margin with a line spacing of 100 m. A 6 km streamer was used, equipped with 240 channels with a group spacing of 25 m. The seismic source used was an array of 14 airguns with a total volume of 4276 in^3. Shot spacing was 50 m, with data being recorded for 12 seconds with a sampling interval of 2ms [*Moore et al.*, 2001a]. Initial data processing was conducted on the *Ewing* and included decimation to 4

ms samples, trace editing, and initial 2D stack and migration. Subsequent data processing was conducted at both the University of Texas and the University of Hawaii. 3D processing consisted of velocity analysis, normal moveout correction, inside and top mute, 3D stack and 3-D post-stack migration. Bin size for the 3D volume is 25 m (inline) by 50 m (crossline). All interpretations used in this study are from 3D time migrated data.

STRUCTURAL OVERVIEW

Tectonic and Stratigraphic Setting

The Nankai accretionary system has been described as an “end-member” convergent margin, due in part to the relative simplicity of the margin’s structure and stratigraphy, and for the almost complete accretion of the incoming sedimentary section [*Shipboard Scientific Party*, 2001]. Subducting oceanic crust in the Moroto area is about 15 Ma in age, and has been interpreted to have formed by back-arc spreading resulting in the creation of the Shikoku Basin [*Hall*, 1995; *Okino et al.*, 1994]. The fossil spreading ridge associated with this process is now oriented roughly perpendicular to the Nankai margin (Figure 2).

Relatively young oceanic crust is overlain by approximately 700 m of hemipelagic sediments (Figure 3). A well at ODP site 1173 (Figure 2) penetrates the entire sedimentary section within the outer trench margin, providing abundant geological data and allowing correlation between seismic data and well logs and cores [*Moore et al.*, 2001b; Mikada *et al*., 2002]. The middle Miocene-Quaternary Shikoku Basin Sequence consists of 688 m of hemipelagic mud and

claystone, and has been divided into Upper and Lower Shikoku Basin facies [*Moore et al.*, 2001b]. Upper Shikoku Basin facies are represented by moderate-amplitude, parallel reflectors correlating to interbedded volcanic ash and tuff layers. Diagenesis has altered these ash and tuff layers to acoustically transparent siliceous claystones in the Lower Shikoku Basin facies [*Moore et al.*, 2001b].

Overlying this basin fill sequence is a ~500 m thick trench fill sequence imaged as an asymmetrical wedge of high-amplitude reflectors onlapping onto the underlying unconformity (Figure 3). This trench-fill sequence was deposited primarily by turbidites transporting terrigenous material derived primarily from uplift and erosion associated with the collision of the Izu-Bonin arc with Honshu to the north (Figure 1), and transported southwest along the margin by trench-axial turbidity flows [*Taira and Niitsuma*, 1985],[Underwood, et al., 1993]. A basal décollement exists within the lower Shikoku Basin sequence. Sediments above this fault are accreted, while lower sediments are initially underthrust. The resulting accretionary prism displays fold-and-thrust style deformation analogous to structures observed in accretionary prisms and mountain belts worldwide [*Davis et al.*, 1983]. The Cascadia accretionary wedge is another sediment-dominated subduction thrust system with highly analogous structures [MacKay, 1995]

Onset of Imbricate Thrusting

Detailed interpretation of reflections at the deformation front document the initiation of fold-and-thrust belt style deformation in a relatively simple tectonic

and stratigraphic setting [*Shipboard Scientific Party*, 2001]. Regularly spaced, seaward-verging imbricate thrusts that sole into a basal décollement are the dominant structural features of the “imbricate thrust zone” that comprises the outermost 20 km of the prism (Figure 2) [*Shipboard Scientific Party*, 2001]. Smaller scale, conjugate back-thrusts are common in this zone, and fault-bend fold hanging wall anticlines develop above imbricate thrusts [*Taira et al.*, 1991]. The onset of this style of deformation occurs in a “protothrust zone” that exists seaward of the frontal thrust, and is characterized by a prominent protothrust, as well as horizontal shortening and structural thickening. [*Moore et al.*, 1990] (Figure 2, 3).

In the protothrust zone several incipient thrusts can be identified in portions of the Shikoku Basin sequence and overlying trench fill (Figure 3, 4). The most prominent of these thrusts (Fault 1 on Figures 3 and 4) is similar in gross geometry to the older thrusts characteristic of the imbricate thrust zone, but exhibits less throw and is discontinuous across the survey area. A low-amplitude hanging wall anticline develops in association with this protothrust, and is expressed on the sea floor as a subtle bathymetric high (Figure 2). This protothrust, and the deformation associated with it, display significant along-strike structural variability across the survey area. The fault is well defined by truncated reflectors in the southwest portion of the survey area. Moving to the northeast the amount of offset varies, and the fault splays into three distinct slip surfaces (Figure 4). Further northeast, offset on all three splays decreases to undetectable amounts. This fault system steps landward and forms a seismically

resolvable fault surface at the northeastern-most portion of the survey area. Hanging-wall anticline development also varies spatially, with areas of more pronounced folding separated by a zone of no detectable folding (Figures 2, 4). Spatial distribution of folding correlates with variations in fault displacement.

NORMAL FAULTING

Fault Geometry

Reflectors of the Upper Shikoku Basin facies and the upper portion of the Lower Shikoku Basin facies are cut by numerous small-offset (20 - 50 m throw) normal faults, represented by truncated and offset reflectors in seismic cross sections (Figures 3-5). As the mean frequency in this interval is about 35 Hz and the velocity is about 1800 m/sec the observed offsets are well above the quarter wavelength of seismic resolution. A horizon representing these faulted sediments was mapped across the survey area. A dip map of this horizon shows numerous discrete, curvilinear zones of high dip (shown in black) separated by nearly flat-lying areas (Figure 6). Zones of high dip correlate to normal faults consisting of 100 – 1000 m segments with complex, intersecting geometries. Other seismic attributes, including amplitude and similarity, were utilized in fault mapping but did not resolve fault geometry better than a simple dip map. Fault density varies across the survey, with zones on higher fault density. Numerous short fault segments with high-angle (~90^{o}) intersections characterize these high fault-density zones.

The contact between the Shikoku basin sequence and overlying trench contact between the Shikoku basin sequence and overlying trench fill turbidites is represented by a continuous, high amplitude, wavy reflector (Figure 3). Overlying reflectors representing trench-fill turbidites onlap onto this reflector and do not appear to be cut by faults (Figure 4). Underlying sediments at the base of the Lower Shikoku Basin facies are imaged as low-amplitude, continuous reflectors that do not appear to be cut by faults [*Moore et al.*, 2001a]. Thus, normal faults are stratigraphically confined to the upper and middle portions of the Shikoku basin sequence.

Oceanic Crust Morphology and overlying Fault Orientations

Oceanic basement underlying the faulted sections is imaged as a high amplitude, semicontinuous reflector in the seawardmost ~40 km of the survey area. This reflector displays elongate horst and graben morphology interpreted as a primary sea floor spreading center fabric (Figure 7). These northwest trending, linear structural highs and lows are on the order of 1 km wide and display up to 200 ms (approximately 175 m) of vertical relief. These features share the same trend as survey shiptracks. Their scale, however, makes it unlikely (but possible) that they are an artifact of data collection or processing. Furthermore, the orientation of this crustal fabric is consistent with the expected orientation of the paleo-spreading center active during the formation of the Shikoku basin [*Le Pichon et al.*, 1987]. This oceanic basement morphology influences normal fault geometry seen in overlying sediments.

Line segments representing 226 km of normal fault traces were digitized within an area of 55 km^2, based on the faulted horizon dip map (Figure 7). An orientation was recorded for every 50 m of these mapped fault traces, so that longer segments could be proportionally weighted in subsequent orientation analysis. Analysis of fault trends reveals a preferential orientation parallel to the margin, or approximately perpendicular to the oceanic basement fabric (Figure 7). Subdivision of digitized fault segments into areas overlying basement highs and lows highlights basement control on fault orientation. Faults overlying basement lows are oriented strongly parallel to the margin trend. Areas overlying basement structural highs, in contrast, have a bimodal distribution of fault trace orientations. Mapped fault traces in these areas show preferential orientations both parallel to, and perpendicular to, the margin (Figure 7). Areas overlying basement structural highs also have a greater density of faulting, with an average of 6.44 km of fault traces per km^2 mapped, verses 2.70 km/ km^2 in areas underlain by basement lows. The correlation between fault orientation and fault density with basement morphology strongly suggests basement control on overlying fault geometry.

Layer-bound Compaction Faults

The observed pattern of normal faulting is notably similar to polygonal fault systems in the North Sea Tertiary interval and elsewhere [*Cartwright and Lonergan*, 1996]. This newly described style of deformation has been attributed to compactive dewatering processes and has been previously documented in 28

localities worldwide, all of which are characterized by very fine-grained sediments [*Cartwright and Dewhurst*, 1998]. The faults observed at Nankai meet several of the criteria Cartwright and Dewhurst use to identify these layer-bound compaction faults: they are polygonal in map view, occur within specific stratigraphic boundaries, are all normal faults with throws of 10 -100 m, and are closely spaced. The Nankai faults differ from other layer-bound compaction fault systems in that they are not organized into “tiers” occupying multiple stratigraphic levels.

North Sea polygonal faults are characterized by typical fault trace lengths (100 – 1000 m) and average throws (30 – 50 m) [*Lonergan et al.*, 1998] that are nearly identical to faults mapped at Nankai. Both sets of faults have complex, intersecting geometries that are polygonal in plan view.

The development of layer-bound compaction faults has been linked to volumetric contraction of fine-grained sediments during early compaction [*Cartwright and Lonergan*, 1996]. Recent work suggests that the colloidal nature of these sediments allows them to behave as gels which contract without evaporation of pore fluid through a process known as syneresis [*Dewhurst et al.*, 1999].

High pore pressures may also play a critical role in the development of layer-bound faulting. Hydrofracturing due to episodic expulsion of fluids from overpressured shales was an early explanation used to explain the lower Tertiary North Sea polygonal faults [*Cartwright*, 1994]. The presence of polygonal faults has been further interpreted as a potential indicator of overpressure in geologic

hazard studies [*Haskel and al.*, 1999]. At Nankai the incoming sedimentary section is loaded by deposition of overlying trench turbidites. This process may generate overpressure within the incoming section and facilitate faulting.

Possible Controls on Fault Orientation

Faults described in the North Sea generally lack the obvious preferred orientations seen at Nankai. Orientations in at least one locality, however, are biased towards paleoslope strike [*Cartwright*, 1994]. The strong margin-parallel preferred orientation observed at Nankai may similarly be related to the landward dip of the Shikoku Basin sequence as it approaches the trench.

The process of differential compaction of fine-grained sediments over irregular topography is known to produce both folding and faulting [*Brown*, 1969; *Labute and Gretener*, 1969]. At Nankai normal faults overlying basement highs display basement fabric-parallel (margin-perpendicular) orientations in addition to margin-parallel preferred orientations. Differential compaction of sediments above basement horsts likely drives the development of faults with the same orientation as basement fabric. The combination of trenchward basement dip and trench-normal basement fabric may thus result in the bimodal orientation distribution of the overlying layer-bound compaction faults.

CONCLUSIONS

This paper describes the seaward limit of deformation at the toe of the Nankai accretionary prism based on interpretation of a 3D MCS survey collected

off Shikoku island, southwest Japan. Data document the initiation of fold-and-thrust belt style deformation, and detailed mapping of the protothrust reveals significant along-strike structural variability.

The 3D geometry of a pattern of normal faults existing seaward of the onset of compressional deformation is described for the first time. Normal faults cut hemipelagic sediments of the incoming Shikoku Basin sequence, and are characterized by a complex, intersecting geometry, which is stratigraphically restricted to a ~500 m thick layer. Faults are preferentially oriented parallel to the trench axis. Sediments overlying basement ridges, however, also contain trench-perpendicular faults that correlate spatially to underlying basement structure. Fault network geometry and basement morphology is resolvable only with quality three-dimensional subsurface imagery.

Observed normal faults are notably similar to layer-bound compaction faults described in lower Tertiary of the North Sea basin, and at least 27 other basins worldwide. These faults have been linked to both volumetric contraction of fine-grained sediments and natural hydrofracturing. Fault development at Nankai is likely influenced by early compactional dewatering processes characteristic of fine-grained sediments, sedimentary loading and burial, basement dip, and basement fabric. The bimodal distribution of preferred orientations observed in layer-bound normal faults seaward of the toe of the Nankai accretionary prism may result from differential compaction above a trenchward dipping basement surface with pronounced trench-normal fabric. Normal faults similar to those described here could explain the earliest tectonic

structures formed in sedimentary sequences of some ancient accretionary prisms [Fisher and Byrne, 1987].

ACKNOWLEDGEMENTS

Support for this work was provided by the National Science Foundation (NSF grant # OCE9802264) and USSP Grant F001431-F001464. Acquisition and processing of 3D MCS data was made possible through the collaborative effort of many, including researchers at the University of Texas, the University of Hawaii, the University of Tokyo, and the Geological Survey of Japan. Seismic interpretation and visualization software was provided by Landmark Graphics Corporation through their university partnership program. Joe Cartwright, Lidia Lonergan, and Ron Nelson made insightful comments regarding fault mapping and structural geology phenomena that proved very helpful. We thank J.R Underhill and I. Cloke for their helpful reviews of the manuscript.

REFERENCES

Ando, M. 1975. Source mechanisms and tectonic significance of historical earthquakes along the Nankai Trough, Japan, Tectonophysics, 27, 119-140.

Ando, M. 1991. A fault model of the 1946 Nankaido earthquake derived from tsunami data, Physics of Earth and Planetary Interiors 28, 320-336.

Aoki, Y., Tamano, T., & Kato, S. 1982. Detailed structure of the Nankai Trough from migrated seismic sections, in Watkins, J. S., and Drake, C. L., eds., Studies in Continental Margin Geology, American Association of Petroleum Geologists Memoir 34, 309-322.

Bradley, D.C., & Kidd, W.S.F. 1991. Flexural extension of the upper continental crust in collisional foredeeps, Geological Society of America Bulletin, 103, 1416-1438.

Brown, P. 1969. Compaction of fine-grained terrigenous and carbonate sediments-a review, Bulletin of Canadian Petroleum Geology, 17, 486-495.

Cartwright, J.A. 1994. Episodic basin-wide fluid expulsion from geopressured shale sequences in the North Sea basin, Geology, 22, 447-450.

Cartwright, J.A., & Dewhurst, D.N. 1998. Layer-bound compaction faults in fine-grained sediments, Geological Society of America Bulletin, 110, 1242-1257.

Cartwright, J.A., & Lonergan, L. 1996. Volumetric contraction during the compaction of mudrocks: a mechanism for the development of regional-scale polygonal fault systems. Basin Research, 8, 183-193.

Davis, D.J., Suppe, J. & Dahlen, F.A. 1983. Mechanics of fold-and-thrust belts and accretionary wedges, Journal of Geophysical Research, 88, 1153-1172.

Dewhurst, D.N., Cartwright, J.A & Lonergan, L. 1999. The development of polygonal fault systems by syneresis of colloidal sediments, Marine and Petroleum Geology, 16, 793 - 810.

Fisher, D., Byrne, T. 1987. Structural evolution of underthrusted sediments, Kodiak Islands, Alaska, Tectonics, 6, 775-794.

Hall, R., Fuller, M., Ali, J.R., & Anderson, C.D. 1995. Active margins and marginal basins of the western Pacific, American Geophysical Union Geophysical Monograph, 88, 371-404.

Haskel, N., et al., Delineation of geologic drilling hazards using 3-D seismic attributes, The Leading Edge, 18, 373-382, 1999.

Karig, D.E. 1986. Physical properties and mechanical state of accreted sediments in the Nankai Trough, S. W. Japan, in: J. C. Moore ed., Structural Fabrics in Deep Sea Drilling Project Cores from Forearcs, Geological Society of America Memoir, 166, 117-133.

Kodaira, S., Takahashi, N., Park, J.O, Mochizuki, K., Shinohara, M. & Kimura, S. 2000. Western Nankai Trough seismogenic zone: Results from a wide-angle ocean bottom seismic survey, Journal of Geophysical Research, 105, 5887-5906.

Labute, G.J., & Gretener, P.E. 1969. Differential compactions around a leduc reef- Wizard Lake area, Alberta, Bulletin of Canadian Petroleum Geology, 17 (3), 304-325.

Le Pichon, X., et al. 1987. Nankai Trough and the fossil Shikoku Ridge: Results of box 6 Kaiko survey, Earth and Planetary Science Letters, 83, 186-198.

Lonergan, L., Cartwright, J. & Jolly, R. 1998. The geometry of polygonal fault systems in Tertiary mudrocks of the North Sea, Journal of Structural Geology, 20, 529 - 548.

MacKay, M. 1995. Structural variation and landward vergence at the toe of the Oregon accretionary prism, Tectonics, 14, 1309-1320.

Mikada, H., Becker, K., Moore, J.C., Klaus, A. et al. 2002. Proceedings of the Ocean Drilling Program, Initial Reports, 196, [CD ROM].

Moore, G.F., Shipley, T.H., Stoffa, P.L., Karig, D.E., Taira, A., Kuramoto, S., Tokuyama, H., & Suyehiro, K. 1990. Structure of the Nankai Trough accretionary zone from multichannel seismic reflection data, Journal of Geophysical Research, 95, 8753-8765.

Moore, G.F., Taira, A., Bangs, N., Kuramoto, S., Shipley, T. (and 15 others), Structural Setting of the Leg 190 Muroto Transect: in: Moore, G.F., Taira, A., Klaus, A., et al., Proc. ODP, Init. Repts., v. 190, Chapter 2, [CD ROM] 2001a.

Moore, G.F., Taira, A., Klaus, A., Becker, K., et. al. 2001b. Proceedings of the Ocean Drilling Program, Initial Reports, 190, [CD ROM]

Moore, G.F., Taira, A., Klaus, A., Becker, L., et. al. 2001c. New insights into deformation and fluid flow processes in the Nankai Trough accretionary prism: Results of Ocean Drilling Program Leg 190, Geochemistry Geophysics and Geosystems 2, 10.129/2001GC000166.

Okino, K., Shimakawa, Y. & Nagaoka, S. 1994. Evolution of the Shikoku Basin, Journal of Geomagnetism and Geoelectricity, 46 (6), 463-479.

Seno, T., Stein, S., & Gripp, A.E. 1993. A model for the motion of the Philippine Sea Plate consistent with NUVEL-1 and geological data, Journal of Geophysical Research, B, Solid Earth and Planets, 98, 17,941-17,948.

Shipboard Scientific Party. 1991. Site 808, pp. 71-269, in Proceedings of the Ocean Drilling Program: Initial Reports, edited by A. Taira, Hill, I. & Firth, J.V., et al., (Ocean Drilling Program), College Station, TX.

Shipboard Scientific Party, Leg 190 Summary. 2001. pp 1-87, in Moore, G.F., Taira, A., Klaus, A., et al., Proceedings of the Ocean Drilling Program: Initial Reports, 190: (Ocean Drilling Program), College Station TX [CD ROM],

Shipboard Scientific Party, Leg 196 Summary. 2002. pp. 1-29, in Mikada, H., Becker, K., Moore, J.C., Klaus, A., et al., Proceedings of the Ocean Drilling Program: Initial Reports, 196: (Ocean Drilling Program), College Station TX [CD ROM].

Taira, A., Hill, I. & Firth, J.V., et al. 1991. Proceedings of the Ocean Drilling Program: Initial Reports, 531 pp., (Ocean Drilling Program), College Station, TX.

Taira, A., & Niitsuma, N. 1985. Turbidite sedimentation in the Nankai Trough as interpreted from magnetic fabric, grain size, and detrital modal analysis, Initial Reports Deep Sea Drilling Project, 87, 611-632.

Underwood, M., Orr, R., Pickering, K., Taira, A. 1993. Provenance and dispersal patterns of sediments in the turbidite wedge of Nankai Trough, in Proceedings of

the Ocean Drilling Program: Scientific Results, edited by Hill, I.A., Taira, A., Firth, J.V., et al., pp 15-33, College Station, TX.

FIGURE CAPTIONS

Figure 1: Regional setting of the Nankai Trough area, including Shikoku island, southwest Japan. Location of study area is outlined in grey. From [*Shipboard Scientific Party*, 2001]

Figure 2: Shaded-relief seafloor depth map from 1999 3D seismic data illustrating the bathymetric expression of various structural domains at the toe of the Nankai accretionary prism. Locations of ODP wells 808i, 1174b,and 1173b are shown.

Figure 3: Seismic and interpretive sections illustrating stratigraphy and structure of the prism toe area. Sections are perpendicular to the trench axis and parallel to the direction of convergence (location shown on figure 2). Fault 1 is the prominent protothrust. Fault 2 is the frontal thrust. Faults 3 and 4 are older in-sequence imbricate thrusts. Numerous small-offset normal faults are visible in the upper and middle portion of the incoming Shikoku Basin sequence.

Figure 4: Perspective view looking NNE of seismic data and interpreted faults and horizons at the prism toe. The vertical dimension is two-way travel time, vertical exaggeration at the seafloor is approximately 5X. The upper surface

represents the seafloor and is shaded by reflection amplitude (yellow/orange = high amplitude, blue/violet = low amplitude). Lower surface represents subducting oceanic basement, shaded by two-way travel time. Fault 1 is the prominent protothrust that bifurcates to form the green and light blue fault splays. Fault 2 is the frontal thrust. Faults 3 and 4 are older in-sequences imbricate thrusts. Normal faults are seen crosscutting the yellow horizon in the incoming sedimentary sequence.

Figure 5: Detailed seismic section of upper and middle Shikoku basin sequence, seaward of the onset of compressional deformation, showing numerous small-offset normal faults. The dashed line is the horizon shown in map view in Figure 6.

Figure 6: Dip map of faulted horizon shown in Figure 4. Dark zones are areas of high dip and correspond to normal fault traces. Heavy black line denotes the frontal thrust trace, with teeth on the overriding accretionary wedge.

Figure 7: Shaded-relief time-structure map of subducting oceanic basement underlying the normal faulted sequence. Heavy red line denotes the frontal thrust trace, with teeth on the overriding accretionary wedge. Thin red lines denote fault segments mapped from dip map (Figure 6). Black lines outline prominent structural trends interpreted to be relict seafloor spreading fabric.

Fault orientations are shown for all faults, faults overlying basement structural highs, and faults overlying basement structural lows.

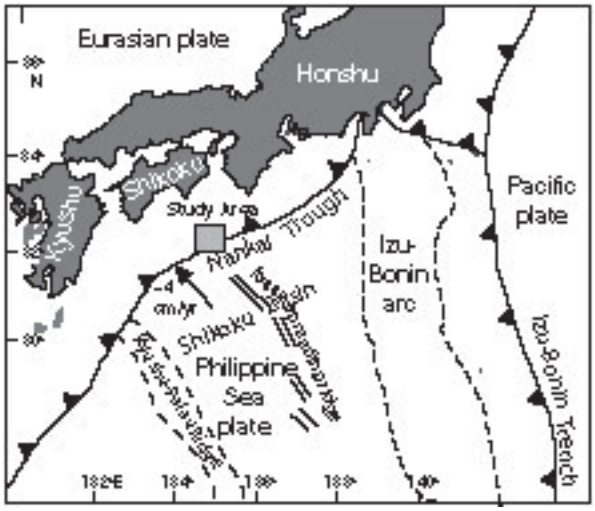
Eurasian plate
Honshu
Shikoku
Kyushu
Study Area
Nankai Trough
Izu-Bonin arc
Pacific plate
Izu-Bonin Trench
Philippine Sea plate
Shikoku
182°E
184°
186°
188°
190°
N

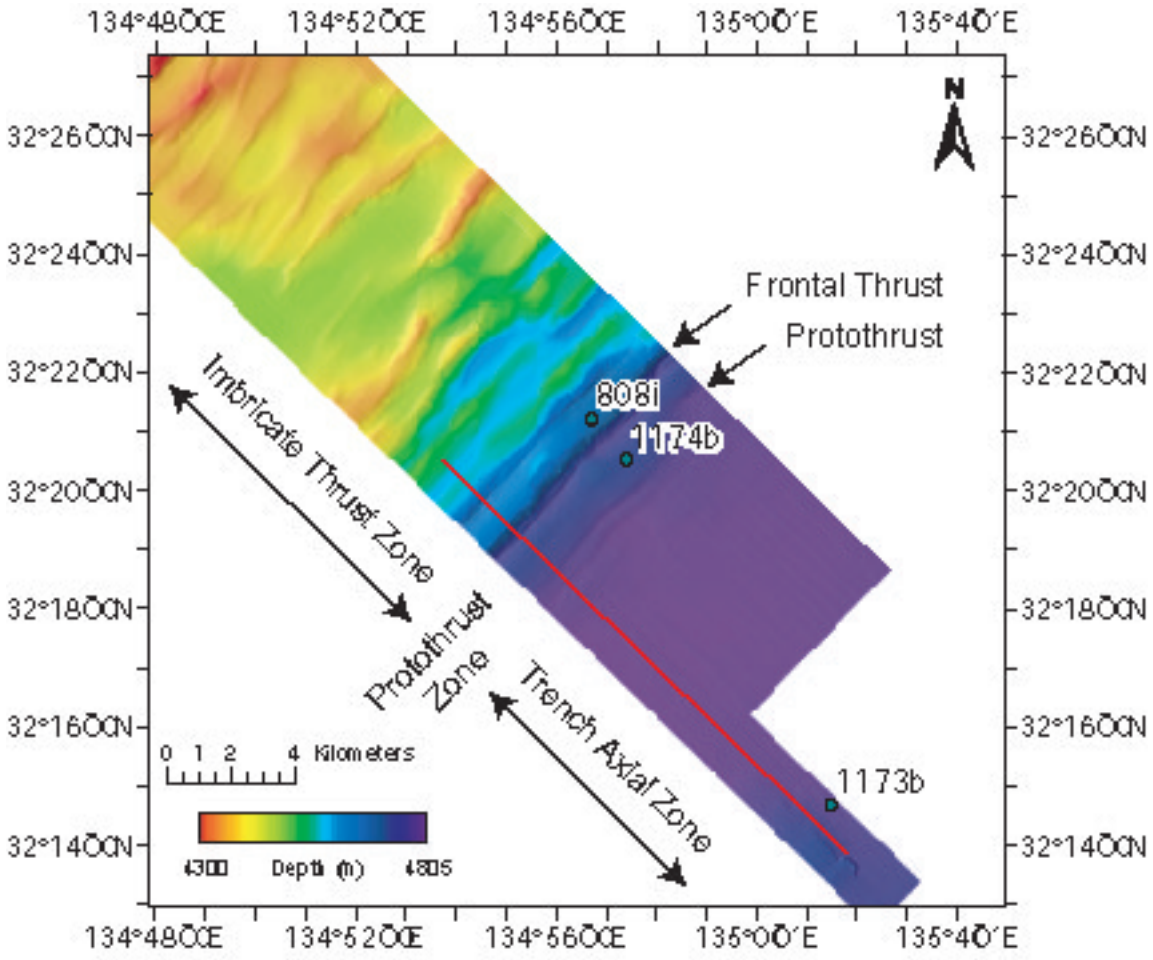
134°48ÕŒE
134°52ÕŒE
134°56ÕŒE
135°0Õ´E
135°4Õ´E
32°26ÕŒN
32°24ÕŒN
32°22ÕŒN
32°20ÕŒN
32°18ÕŒN
32°16ÕŒN
32°14ÕŒN
N
Frontal Thrust
Protothrust
808I
1174b
1173b
Imbricate Thrust Zone
Protothrust Zone
Trench Axial Zone
0 1 2 4 Kilometers
4300 Depth (m) 4805

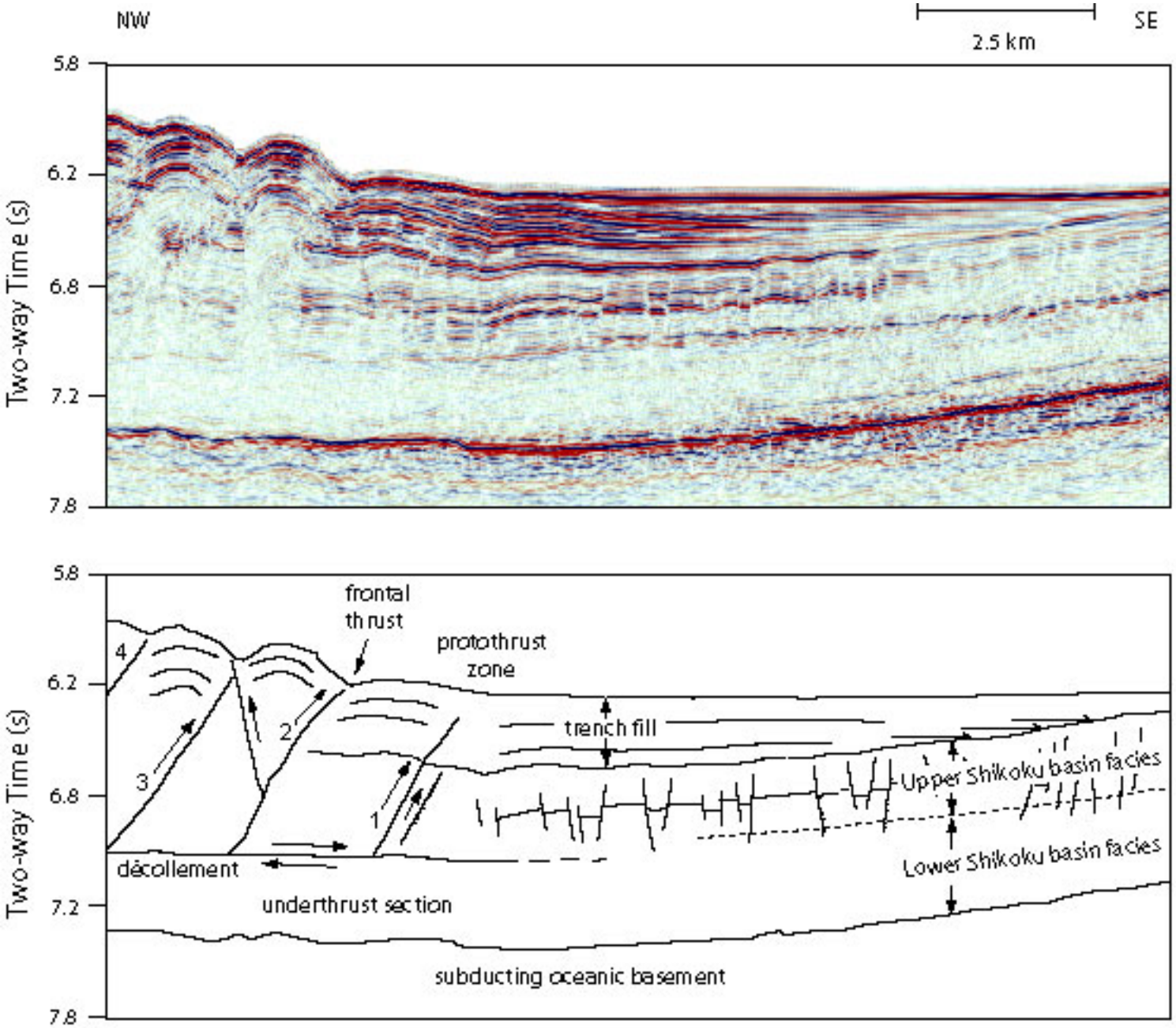
NW
SE
2.5 km
Two-way Time (s)
5.8
6.2
6.8
7.2
7.8
frontal thrust
protothrust zone
trench fill
Upper Shikoku basin facies
Lower Shikoku basin facies
décollement
underthrust section
subducting oceanic basement
1
2
3
4

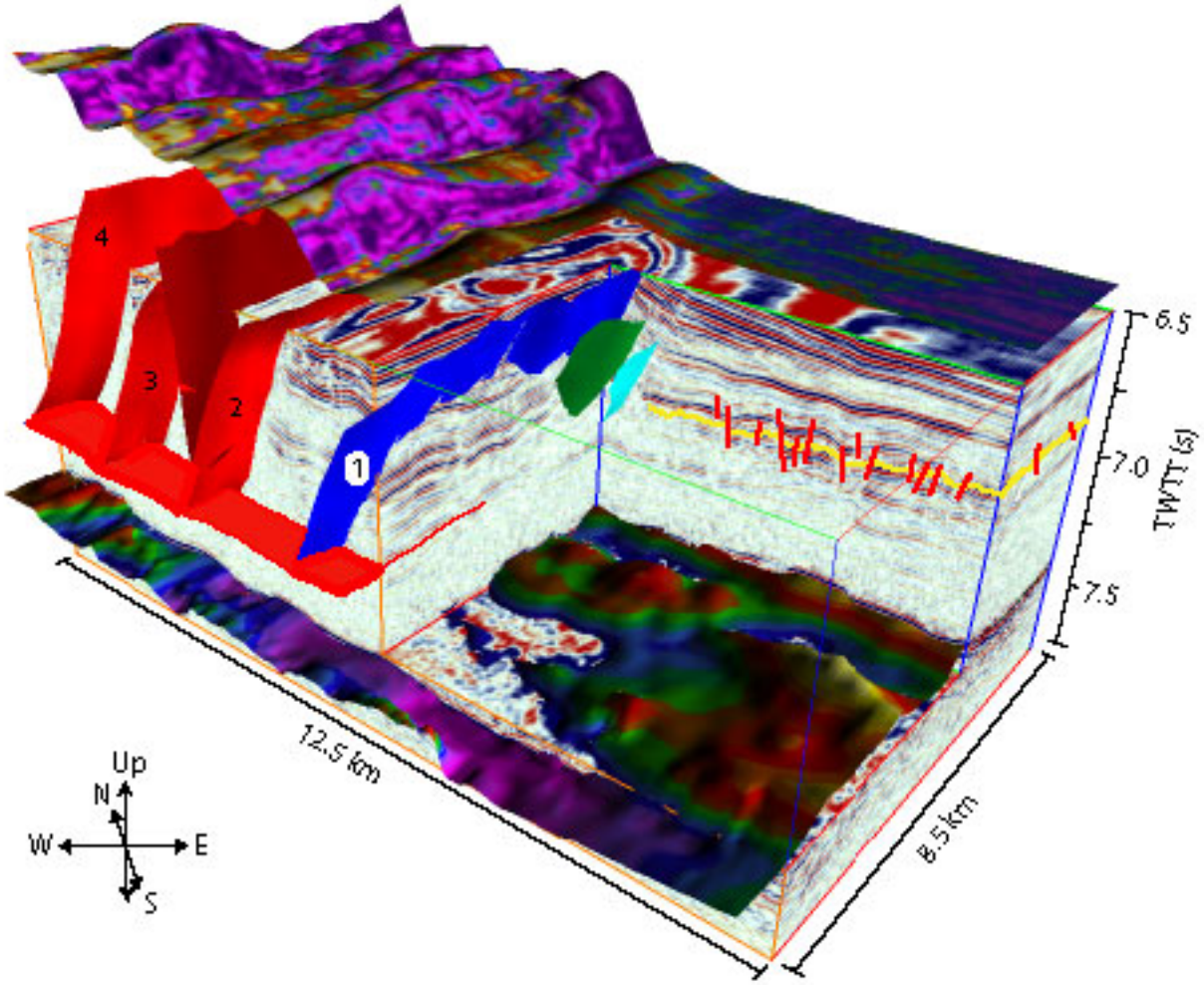
4
3
2
1
6.5
7.0
7.5
TWTT (s)
12.5 km
8.5 km
Up
N
W
E
S

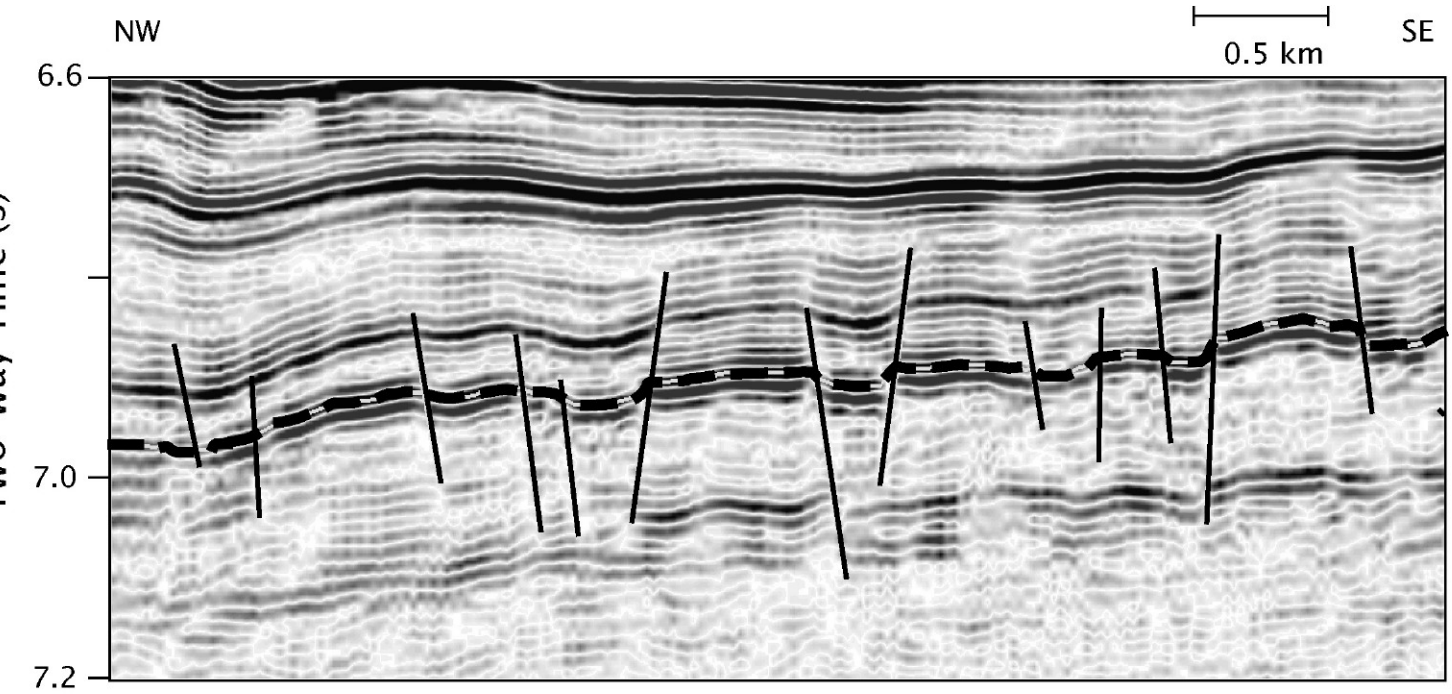
NW
SE
0.5 km
6.6
7.0
7.2

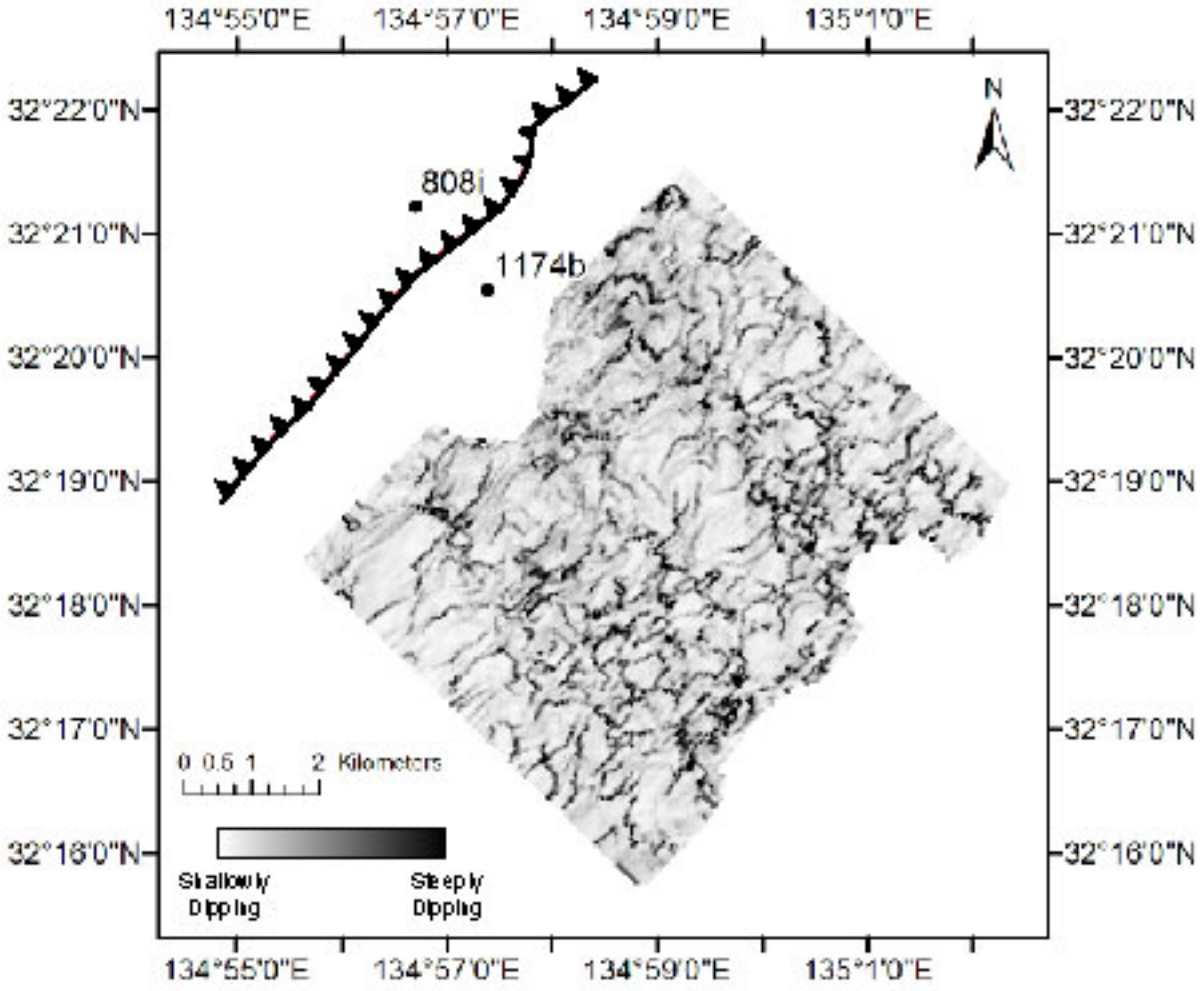
134°55'0"E
134°57'0"E
134°59'0"E
135°1'0"E
32°22'0"N
32°21'0"N
32°20'0"N
32°19'0"N
32°18'0"N
32°17'0"N
32°16'0"N
N
808j
1174b
0 0.5 1 2 Kilometers
Shallowly Dipping
Steeply Dipping

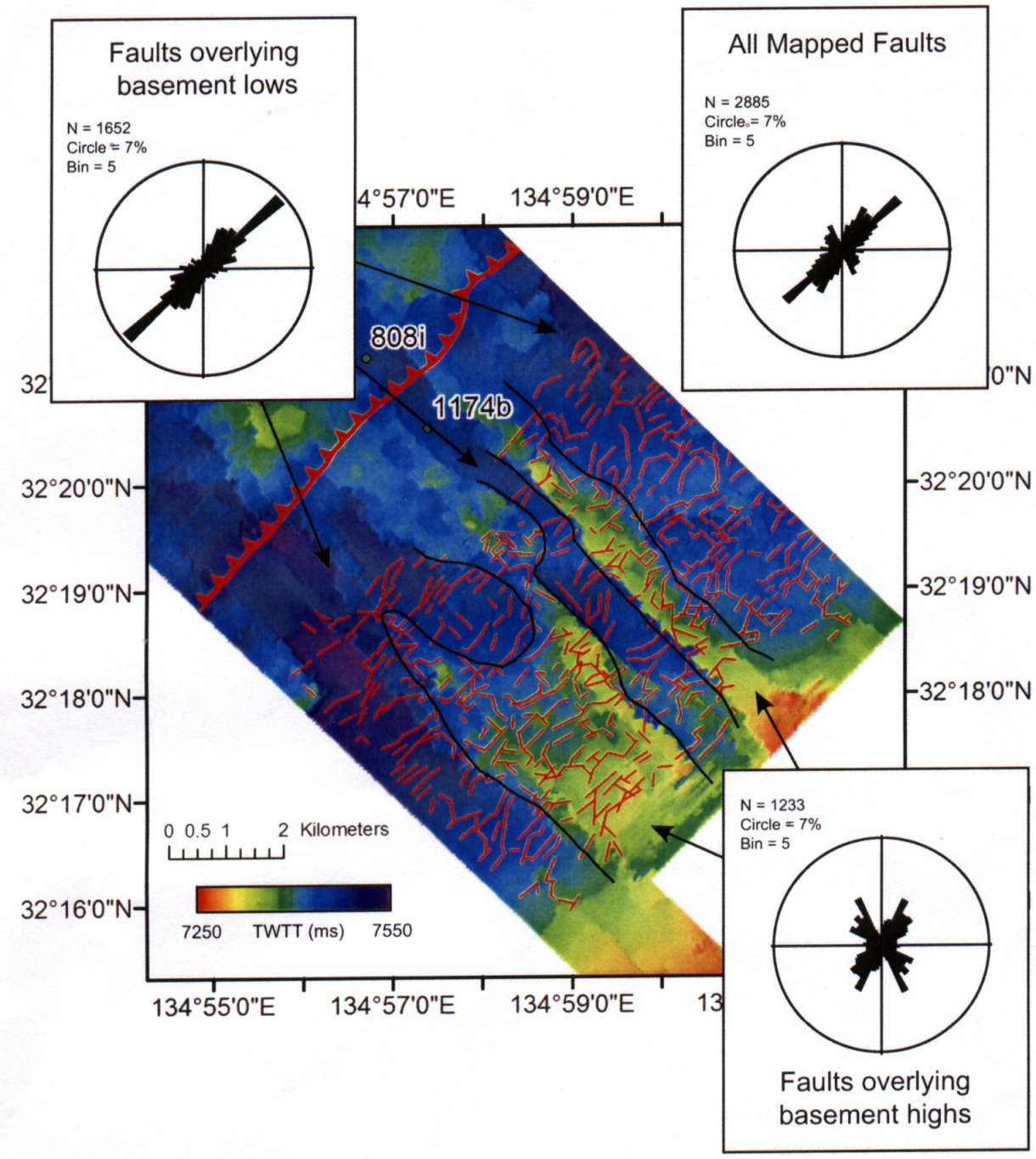
Faults overlying basement lows
N = 1652
Circle = 7%
Bin = 5
All Mapped Faults
N = 2885
Circle = 7%
Bin = 5
808i
1174b
134°57'0"E
134°59'0"E
32°20'0"N
32°19'0"N
32°18'0"N
32°17'0"N
32°16'0"N
0 0.5 1 2 Kilometers
7250 TWTT (ms) 7550
134°55'0"E
134°57'0"E
134°59'0"E
N = 1233
Circle = 7%
Bin = 5
Faults overlying basement highs